

Network inference using asynchronously updated kinetic Ising Model

Hong-Li Zeng,^{1,*} Erik Aurell,^{2,3} Mikko Alava,¹ and Hamed Mahmoudi³

¹*Department of Applied Physics, Aalto University, FIN-00076 Aalto, Finland*

²*Linnaeus Centre, KTH-Royal Institute of Technology, SE-100 44 Stockholm, Sweden*

³*Department of Information and Computer Science, Aalto University, FIN-00076 Aalto, Finland*

(Dated: November 3, 2018)

Network structures are reconstructed from dynamical data by respectively naive mean field (nMF) and Thouless-Anderson-Palmer (TAP) approximations. For TAP approximation, we use two methods to reconstruct the network: a) iteration method; b) casting the inference formula to a set of cubic equations and solving it directly. We investigate inference of the asymmetric Sherrington-Kirkpatrick (S-K) model using asynchronous update. The solutions of the sets cubic equation depend of temperature T in the S-K model, and a critical temperature T_c is found around 2.1. For $T < T_c$, the solutions of the cubic equation sets are composed of 1 real root and two conjugate complex roots while for $T > T_c$ there are three real roots. The iteration method is convergent only if the cubic equations have three real solutions. The two methods give same results when the iteration method is convergent. Compared to nMF, TAP is somewhat better at low temperatures, but approaches the same performance as temperature increase. Both methods behave better for longer data length, but for improvement arises, TAP is well pronounced.

PACS numbers: 02.50.Tt, 02.30.Mv, 89.75.Fb, 87.10.Mn

I. INTRODUCTION

A present challenge in biological research is how to deal with the data originating from the high-throughput technologies. Information can often convincingly be structured in the form of networks [1]. Vertices on a network are entities and the links with numbers or other descriptions attached to them are the interactions between the elements, in, e.g., the biological system [2–5]. On different levels of abstraction, information about the interactions between each pair of elements is hence useful to understand the biological system. Finding interactions between entities from the empirical data is an inverse problem called ‘network reconstruction’ [1, 6, 8, 11–13].

In this work, we use an idealized system to generate ‘empirical’ data with computer, and then try to reconstruct the network structure of the system, using this test data. The system is the kinetic Ising model, intended as a proxy for simultaneous recordings from many neurons. In this setting, symmetric couplings between the entities are not appropriate, since two neurons will typically not act on each other in a symmetric way [15]. The properties of asymmetric neural networks have been studied previously [16–18], but not much work has been done in the context of network reconstruction. Here we extend a presently reported approach using dynamic mean field theory [10, 29] from synchronously updated models to asynchronously updated models. The analysis closely parallels that of [29], with the difference that data is continuous in time. The similarities and differences between our results and [29] are commented upon in Conclusion.

Multi-neuron firing patterns can be observed with

present technologies up to thousands of neurons (recordings on retina systems). Schneidman et al. [7] showed that the interactions between neuron pairs could be reconstructed using only the observed firing rates and the pair-wise correlations. Recently, questions have arisen whether the methods used in [7] generalize to other data sets, and if the approximations involved can be improved or not [8, 11–13]. There has also been significant development on the more theoretical side [8, 14, 27, 28].

A theoretical model, which can be used to generate the frequencies of all possible spiking configurations is the well-known Ising model [8]. For a system of N neurons, it is characterized by up to N^2 parameters: N external fields, θ_i , on each individual neuron, and $N(N-1)$ ‘links’, J_{ij} , between each pair of neurons. In the asymmetric Ising model, J_{ij} is not equal to J_{ji} . And for S-K model, the symmetrized and anti-symmetrized couplings J_{ij}^s and J_{ij}^{as} are identically independent Gaussian distributed random variables. The model is entitled ‘kinetic’ because, except for the fully symmetric case, it does not correspond to an equilibrium statistical mechanics system.

With the observed average firing rates and all pairwise equal-time correlations in an empirical data set, maximum entropy models can find a probability distribution which maximizes the entropy of the data domain. This condition implies that the samples are drawn independently from the same distribution. The state of maximum entropy given is an equilibrium state which has a probability distribution of Ising form [9]. The quantities J_{ij} and h_i are then Lagrange multipliers to satisfy the constraints that the ensemble expectation values agree with sample averages in the data set. If the data is however generated by a dynamics, then samplings drawn close in time are typically dependent. This is the extra information which will be used here through the kinetic inverse Ising reconstruction scheme. For the equilibrium

*Email address: hongli.zeng@tkk.fi

version of the inverse Ising problem, Yasser Roudi and collaborators review and investigate several approximation methods [11, 12, 28] with the maximum entropy method, arriving at the general conclusion that all of them are unreliable in a dynamic setting, if the systems are sufficiently large, and in most ranges of parameters. Better inference methods on dynamic data are called for.

A standard approach to sample the equilibrium Ising model is Glauber dynamics, which we will describe below. It is however not restricted to symmetric Ising model, but also well-defined for models with asymmetric couplings. It is plausible that such a more general framework can describe the underlying system not close to equilibrium, and with asymmetric couplings, better. Here we are therefore interested in using kinetic Ising model, typically with asymmetric couplings, to reconstruct a neural network dynamically.

There are several reasons to consider asynchronous update models (Glauber dynamics) instead of synchronous update. The first is that asynchronous updates converge to a stationary state which for symmetric models in the Boltzmann-Gibbs equilibrium measure, while neither is necessarily true for synchronous updates. A second reason is that most plausible applications are naturally asynchronous. For instance, the expression of gene is not a synchronous process, the transcription of DNA and the transport of enzymes may take from milliseconds up to a few seconds. Another example is the refractory period for neuron in which the neuron cannot respond to input signal as it is still processing or recovering from the previous input signal. The period generally lasts for one millisecond [19]. Besides, [20, 21] show that the biological networks do not have a completely synchronous update. For these reasons, we have focused on the asynchronous update Glauber dynamics. For a discussion of synchronous update we refer to [10, 29].

The paper is organized as follows: we describe the asymmetric S-K model and Glauber dynamics in Sec. II; the inference formula with nMF and TAP approximation for asynchronous case is derived in Sec. III; the performances of the inference formula are given in Sec. IV. Finally, we summarize the work in Sec. V.

II. ASYMMETRIC S-K MODEL AND GLAUBER DYNAMICS

The S-K model is a system of N spins, which models N neurons with binary states ($s_i = 1$ for firing state, otherwise $s_i = -1$). It is a fully connected model, i.e., all neurons in the system have interactions with each other. The interactions J_{ij} between each pair of neurons have the following form:

$$J_{ij} = J_{ij}^s + kJ_{ij}^{as}, \quad k \geq 0. \quad (1)$$

where, k measures the asymmetric degree of these interactions, J_{ij}^s and J_{ij}^{as} are symmetric $J_{ij}^s = J_{ji}^s$ and asymmetric matrices $J_{ij}^{as} = -J_{ji}^{as}$, respectively. They

consists both of identically and independently Gaussian distributed random variables with means 0 and variances:

$$\langle J_{ij}^{s2} \rangle = \langle J_{ij}^{as2} \rangle = \frac{J^2}{N} \frac{1}{1+k^2}. \quad (2)$$

The self-connections are avoided, i.e., the on-diagonal elements of J_{ij}^s and J_{ij}^{as} equals 0.

We now define the kinetic Ising model with asynchronous updates. Let the joint probability distribution of spin states in system at time t as $p(s_1, \dots, s_N; t)$, and let the master equation of our model be written as

$$\begin{aligned} & \frac{d}{dt} p(s_1, \dots, s_N; t) \\ &= \sum_i \omega_i(-s_i) p(s_1, \dots, -s_i, \dots, s_N; t) - \sum_i \omega_i(s_i) p(s; t). \end{aligned} \quad (3)$$

where $\omega_i(s_i)$ is the flipping rate, i.e., the probability for the state of i th neuron changes from s_i to $-s_i$ per unit time. The flipping rates are given by Glauber dynamics as follows:

$$\omega_i(s_i) = \frac{1}{1 + \exp[2\beta s_i(\theta_i + \sum_j J_{ij} s_j)]}. \quad (4)$$

where, β is the inverse of temperature T . For convenience, define $H_i = \sum_j J_{ij} s_j + \theta_i$ as the effective field on neuron i , where θ_i is the external field of spin i . If the couplings are symmetric (i.e., $J_{ij}^{as} = 0$), then the steady state of the dynamics given by (3) and (4) is $p(s_1, \dots, s_N) \propto \exp(\beta \sum_i s_i \theta_i + \sum_{ij} s_i s_j J_{ij})$. If the couplings are not symmetric, then (3) and (4) still have a steady state (under general condition), but this state does not have a simple description.

With state for each neuron s_i , we can naturally define the time dependent means and correlations as follows:

$$\begin{aligned} m_i &= \langle s_i(t) \rangle. \\ C_{ij}(t - t_0) &= \langle s_i(t) s_j(t_0) \rangle - m_i m_j. \end{aligned} \quad (5)$$

From equation (3) and (4), we get the equation of motion for means and correlations as

$$\begin{aligned} & \frac{dm_i}{dt} = m_i + \langle \tanh[\beta s_i H_i(t)] \rangle. \\ & \frac{d}{dt} \langle s_i(t) s_j(t_0) \rangle = -\langle s_i(t) s_j(t_0) \rangle + \langle \tanh[\beta H_i(t) s_j(t_0)] \rangle. \end{aligned} \quad (6)$$

For the second equation of eq. (6), the term in the left hand side and the first term in the right hand side can be solved based on the empirical data produced by the Glauber dynamics. However, the calculation of the average value for $\tanh[\beta H_i(t) s_j(t_0)]$ involves all kinds of higher-order correlations and is therefore not easily expressed only in terms of means and pair-wise correlations. In order to solve the second equation in (6), perturbatively approximations for the second term of the right hand side are obviously needed. Here, we use the nMF and TAP approximations respectively to deal with this **tanh** function.

III. NMF APPROXIMATION AND TAP APPROXIMATION

The simplest method to find out the parameters of the Ising model from empirical data is the mean-field theory:

$$m_i = \tanh\beta(\theta_i + \sum_j J_{ij}m_j) \quad (7)$$

Following recent practice, and to distinguish this first level of approximation from others, we will refer to it as naive mean-field (nMF). Let $b_i = \theta_i + \sum_j J_{ij}m_j$ and rewrite H_i as

$$H_i = b_i + \sum_j J_{ij}(s_j - m_j) \equiv \sum_j J_{ij}\delta s_j + b_i. \quad (8)$$

Expanding the **tanh** function with respect to βb_i in equation (6)

$$\begin{aligned} & \frac{d}{dt}\langle s_i(t)s_j(t_0) \rangle + \langle s_i(t)s_j(t_0) \rangle \\ &= m_i m_j + \beta(1 - m_i^2) \left(\sum_k J_{ik} \langle \delta s_k(t) \delta s_j(t_0) \rangle \right). \end{aligned} \quad (9)$$

and denoting the time difference $t - t_0$ as τ , we have

$$\frac{d}{d\tau} C_{ij}(\tau) + C_{ij}(\tau) = \beta(1 - m_i^2) \sum_k J_{ik} C_{kj}(\tau). \quad (10)$$

In the limit $\tau \rightarrow 0$, we obtain the equation which we need to infer the network couplings:

$$J = TA^{-1}DC^{-1}. \quad (11)$$

where $D = \dot{C} + C$ and $A_{ij} = \delta_{ij}(1 - m_i^2)$.

Equation (11) is a linear matrix equation with respect to J_{ij} . We can solve it directly.

Next, we turn to derive the inference formula with TAP approximation. If the Onsager term, i.e., the effect of the mean value of neuron i on itself via its influence on another neuron j , is taken into account, the TAP equation is [26]

$$m_i = \tanh(\beta b_i - m_i \beta^2 \sum_{k \neq i} J_{ik}^2 (1 - m_k^2)). \quad (12)$$

With

$$T_i = b_i \pm m_i \beta^2 \sum_{k \neq i} J_{ik}^2 (1 - m_k^2) + \sum_j J_{ik} \delta s_k. \quad (13)$$

and eq. (12), we expand the **tanh** function in eq. (6) with respect to

$$\beta b_i - m_i \beta^2 \sum_{k \neq i} J_{ik}^2 (1 - m_k^2)$$

to the third order and keep the terms only up to the third of \mathbf{J} . Then the corresponding TAP inference formula for

J_{ij} is obtained, which is formally the same as in the nMF approximation.

$$J = TA^{-1}DC^{-1}. \quad (14)$$

However, matrix \mathbf{A} in TAP formula is different

$$A_{ij} = \delta_{ij}(1 - m_i^2) \left[1 - \beta^2(1 - m_i^2) \sum_j J_{ij}^2(1 - m_j^2) \right]. \quad (15)$$

Eq. (14) is a function of the couplings \mathbf{J} , and therefore it is a nonlinear equation for matrix \mathbf{J} .

We try to solve eq. (14) for \mathbf{J} though two approaches. One way is to solve it iteratively. We start from reasonable initial values J_{ij}^0 and insert them in the right hand side of the formula. The resulting J_{ij}^1 is the solution after one iteration. This can be again replaced in the right hand side to get the second iteration results and etcetera ...

$$J^{t+1} = TA(J^t)^{-1}DC^{-1} \quad (16)$$

An alternative way is solving it directly, as done for the synchronous update model in [29], casting the inference formula to a set of cubic equations. For eq. (15), we denote

$$F_i = \beta^2(1 - m_i^2) \sum_j J_{ij}^2(1 - m_j^2) \quad (17)$$

and plug it into eq. (14), and then obtain the following equation for J_{ij} :

$$J_{ij}^{\text{TAP}} = \frac{T * V_{ij}}{(1 - m_i^2)(1 - F_i)} \quad (18)$$

where $V_{ij} = [DC^{-1}]_{ij}$. Inserting eq. (18) into eq. (17), we obtain the cubic equation for F_i as:

$$F_i(1 - F_i)^2 - \frac{\sum_j V_{ij}^2(1 - m_j^2)}{1 - m_i^2} = 0. \quad (19)$$

With the obtained physical solution for F_i , we get the reconstructed couplings J^{TAP} as

$$J_{ij}^{\text{TAP}} = \frac{J_{ij}^{\text{nMF}}}{1 - F_i}. \quad (20)$$

It is worth mentioning that for the cubic equation (18), we have three solutions with possible imaginary parts. Here we study the real roots of the cubic equation and ignore those solutions with imaginary parts. When three solutions are all real ones, we take the smallest one.

We introduce Δ to measure the difference between the reconstructed network structure and the original true ones, i.e., Δ is the reconstruction error

$$\Delta = \sqrt{\frac{\sum_{i \neq j} (J_{ij}^{\text{re}} - J_{ij}^{\text{t}})^2}{\sum (J_{ij}^{\text{t}})^2}}.$$

where J_{ij}^{t} represents the true network couplings and J_{ij}^{re} for the reconstructed ones.

IV. THE PERFORMANCES OF NMF AND TAP APPROXIMATION

As the starting point, we take a look at the number of solutions given by nMF and TAP approximation. The nMF gives unique solution while the iteration method of TAP starting from nMF provides 0 solution when the iteration is divergent and 1 solution for convergence. However, the cubic-equation method of TAP approximation always contains at least one solution. Denote the constant term of eq. (19) as x ,

$$x = -\frac{\sum_j V_{ij}^2(1 - m_j^2)}{(1 - m_i^2)} \quad (21)$$

x is temperature dependent and negative as $0 < m_i^2 < 1$. The cubic equation (19) has 3 real roots when $-\frac{4}{27} < x < 0$. We only consider the smallest one and indeed it provides the most accurate J_{ij} 's (data are not shown). With $x < -\frac{4}{27}$, eq. (19) has only one real root and other two complex solutions with imaginary part which are discarded as they have no physical meaning. In Fig. 1, we give the fraction of cubic-equation set (19) (as $i = 1, 2, \dots, N$, where N is the system size) which contains three real solutions. When the set of cubic-equation at given T contains N real and $2 * N$ complex solutions, we say the fraction of three real roots equals 0 at this temperature point. As shown in Fig. 1, a transition seems to occur around $T_c = 2.1$. For large system size and $T < 2.1$, the solutions for eq. (19) has only one real root while for $T > 2.1$ 3 real ones. We plot this figure for data length $L = N * 10^6$, so smaller N means shorter data length, that explains why the curve of $N = 20$ is not quite smooth.

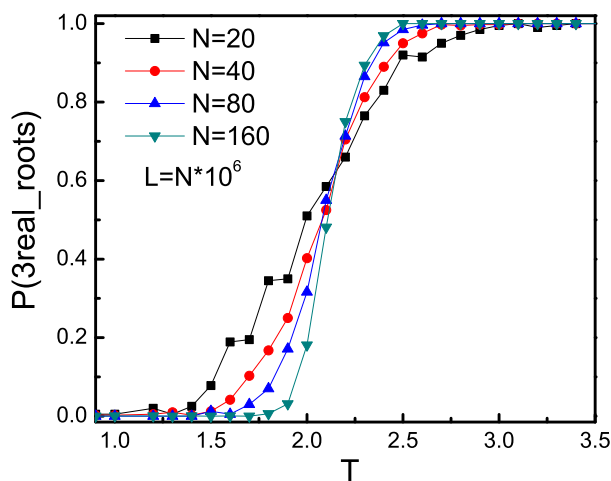


FIG. 1: (Color online) The fraction of 3 real roots for the cubic equation set eq. (19). A transition seems to occur around $T_c = 2.1$. Here, we find larger N , the transition curve sharper. The parameter values: $\theta = 0.5$, $k = 1$, $L = 20 * 10^6$.

For the simulation of the iteration method of TAP approximation, we take the reconstructed J_{ij}^{MF} by nMF as

the initial input J_{ij}^0 , and follow eq. (16) to get $J_{ij}^1, J_{ij}^2, \dots$ iteratively. If the average value of $\delta(t) = |J_{ij}^t - J_{ij}^{t-1}|$ less than the threshold value 10^{-5} , then, we consider the iteration is convergent and stop iteration. An interesting phenomena of the iteration method is it is divergent when the solutions of cubic-equation set contain complex roots while convergent when they contain only real roots. Here, we mention three possible causes for the divergence. One originates from the frozen states of spin-glass where $m_i^2 = 1$ and neither nMF nor TAP can work. A second possible cause: there exists a single fixed point of the solution but the initial J_{ij} 's are drawn as J_{ij}^{MF} , which may a little bit far away from the true solutions for J_{ij} 's at low T , and the iteration can not reach to the fixed point. The last possible cause may come from the fixed point which is unstable. Here, the given results are for $\theta = 0$ and $k = 1$, there is no frozen states for the given temperatures. Then, the divergence may arise by the second or third possible reason.

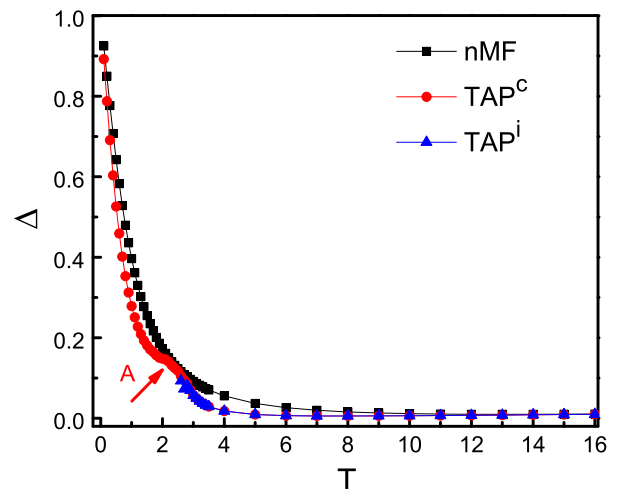


FIG. 2: (Color online) The reconstruction error Δ with temperature T for both nMF and TAP approximation. The other parameter values: $N = 20$, temperature $L = 20 * 10^{10}$, external field $\theta = 0$, asymmetric degree $k = 1$. Notations: black square for nMF red circle for cubic equation method for TAP, blue triangle for iteration method for TAP. Each data point is averaged on 10 realizations.

We next turn to investigate the influence of T on the reconstruction errors Δ in the case of zero external field ($\theta = 0$) aS-K model ($k = 1$). We plot Δ with T for nMF and TAP in Fig. 2. For TAP approximation, when iteration method is convergent, it produces the same results (blue triangle) as the cubic-equation method (red circle). Both approximations work better with temperature T increasing but approach to the same behavior when T goes higher. It is because for eq. (15), the Onsager term will approach 0 if T goes high enough, i.e., there will be no difference between nMF and TAP approximation. As shown in Fig. 2, TAP always works better than nMF before they approach to the same results. But there is

an noticeable area in which the curve by the cubic equation method of TAP pointed to with letter 'A' is not as smooth as that of nMF. The reason is this temperature interval is located in the critical area where the solutions of the cubic-equation set eq. (19) are coexistence of two states: some spins have 3 real roots and the others have only 1 real root. We tested also for systems with different size and found that larger system size give more clear inflexions and closer to the critical temperature T_c , around 2.1. Such results are consistent with the results shown in Fig. 1.

Fig. 3 illustrates the reconstructions errors for every J_{ij} 's with scatter plots of the inferred J_{ij} 's by nMF and TAP approximation against J_{ij}^{true} 's. The left plot is for the data length $L = N * 10^5$ and $L = N * 10^7$ for the right one. Here, the system size $N = 20$ and the temperature $T = 3.7$ for this plot where the iteration method of TAP is convergent. The scatter plot shows that both nMF and TAP perform better for larger L . As shown in both left and right hand side of Fig. 3, the data points for J_{ij}^{TAP} 's inferred by cubic-equation method are almost covered by that for J_{ij}^{TAP} 's inferred by iteration method, especially for $L = N * 10^7$.

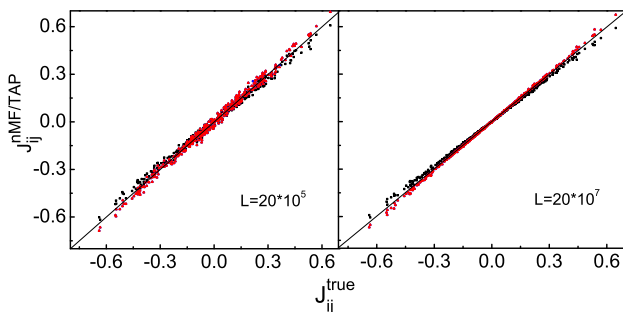


FIG. 3: (Color online) The scatter plot for the reconstructed couplings versus the true ones. The parameter values: $N = 20$, temperature $T = 3.7$, external field $\theta = 0$, asymmetric degree $k = 1$. Notations: black square for inferred couplings using nMF versus J_{ij}^{true} , blue circle for iteration equation method of TAP versus J_{ij}^{true} , red triangle for cubic method of TAP versus J_{ij}^{true} .

From the right plot in Fig. 3, it is difficult to say which approximation is better as the reconstruction error is quite small especially with longer data length. Thus, we move next to see how the data length L works on the reconstruction error Δ in the case of zero external field aSK model. With the asynchronously updating Glauber dynamics, longer data length L ($L = N * L'$, where L' is the data length in the corresponding synchronous update case, N is the system size) is needed to obtain comparable results with that in synchronous case [29] and say something about our system. In Fig. 4, Δ versus L for both nMF and TAP are plotted for a given temperature $T = 8$, where the iteration method of TAP is convergent. They both reconstruct better with increasing L , i.e., Δ decreases as L increases. For short data length

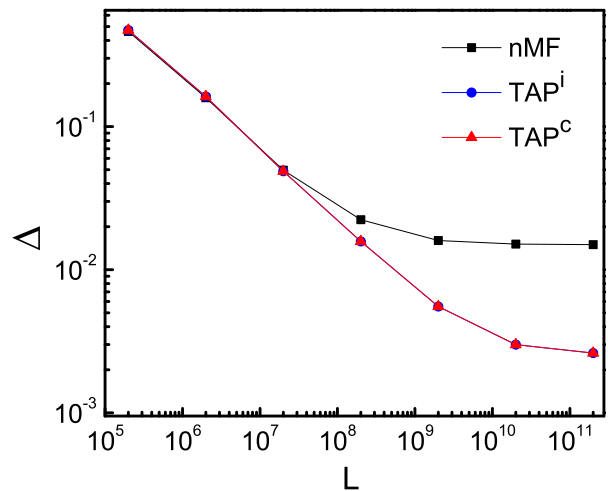


FIG. 4: (Color online) Reconstruction error Δ versus the data length L for nMF and TAP approximation. The other parameter values: $N = 20$, temperature $T = 8$, external field $\theta = 0$, asymmetric degree $k = 1$. Notations: black square for nMF, blue circle for iteration equation method of TAP, red triangle for cubic method of TAP.

$L < N * 10^7$, nMF and TAP produce almost the same reconstruction error. However, TAP works better than nMF when $L > N * 10^8$. The Δ for TAP is one order smaller than that for nMF when $L \geq N * 10^9$. Here, again, we find the data points for cubic-equation method of TAP are covered by those for iteration method of TAP.

The above results are general to different system size N . The performances for nMF and TAP are also compared with non-zero external field $\theta \neq 0$. We find there exists a frozen state in the low testing temperature where neither nMF nor TAP can work there.

V. CONCLUSION

We studied the network inference using asynchronously updated kinetic Ising model. Two approximations, nMF and TAP, are introduced to infer the connections and connection strengths in the network. We have found the transition of the solutions' type for the cubic equation method of TAP with critical temperature $T_c \approx 2.1$. We have implemented the TAP approximation as two different schemes, the cubic scheme, and the iteration scheme. For large system, the T_c seems to be the starting temperature point for TAP iteration method to converge.

Comparing our work with [29] in which the synchronously updated Glauber dynamics is used, we find two similarities. The first one is both approximations reconstruct better with increasing temperature or longer data length. The other one is TAP works better than nMF especially with long data length at given temperatures. There are also differences. For instance, the improvement by TAP approximation in asynchronous case

is not as much as that in synchronous case. Besides, in order to get the comparable results with synchronous case, the data length for asynchronous case should be at least N times longer than that for synchronous case.

This work is able to extend to deal with the biological data from experiments, especially for data produced in continuous time which correspond to the asynchronous updates. Given the large amount of data needed to see a difference, we believe that in most application scenarios, network inference using asynchronously updated kinetic Ising models should work well enough using naive mean-field (nMF) reconstruction, and the further step to TAP

reconstruction would not be needed.

Acknowledgements

We are grateful to J. Hertz and Y. Roudi for useful discussions about the work and Nordita for hospitality. The work of H.-L. Z., E. A., and H. M. was supported by the Academy of Finland as part of its Finland Distinguished Professor program, project 129024/Aurell.

-
- [1] J. J. Rice, Y. Tu, G. Stolovitzky, *Bioinformatics* **21**, 765 (2005).
- [2] K. W. Kohn, *Mol. Biol. Cell* **10**, 2703 (1999).
- [3] L. H. Hartwell, J. J. Hopfield, S. Leibler and A. W. Murray, *Nature* **402**, C47 (1999).
- [4] U. S. Bhalla and R. Iyengar, *Science* **283**, 381 (1999).
- [5] H. Jeong, B. Tombor, R. Albert, Z. N. Oltvai, A.-L. Barabasi, *Nature* **407**, 651 (2000).
- [6] T. S. Gardner, D. di Bernardo, D. Lorenz, J. J. Collins, *Science* **301**, 102 (2003).
- [7] E. Schneidman, M. Berry, R. Segev, W. Bialek, *Nature* **440**, 1007 (2006).
- [8] S. Cocco, S. Leibler, R. Monasson, *Proc. Natl. Acad. Sci. U.S.A.* **106**, 14058 (2009).
- [9] C. E. Shannon, *Bell. Syst. Tech. J.* **27**, 379 (1948).
- [10] J. A. Hertz *et al*, *BMC Neuroscience* **11**, (Suppl): 51 (2010)
- [11] Y. Roudi, J. A. Hertz, E. Aurell, *Front. Comput. Neurosci.* **3**, 1 (2009).
- [12] Y. Roudi, S. Nirenberg, P. E. Latham, *PLoS Comput. Biol.* **5**, e1000380 (2009).
- [13] Y. Roudi, J. Tyrcha, J. Hertz, *Phys. Rev. E* **79**, 051915 (2009).
- [14] M. Mezard and T. Mora, *J. Physiol. Paris* **103**, 107 (2009).
- [15] H. Sompolinsky and I. Kanter, *Phys. Rev. Lett.* **57**, 2861 (1986).
- [16] M. V. Feigelman and L. B. Ioffe, *Int. J. Mod. Phys. B* **1**, 51 (1987).
- [17] R. Bausch, H. K. Janssen, R. Kree, A. Zippelius, *J. Phys. C.* **19**, L779 (1986).
- [18] G. Parisi, *J. Phys. A* **19**, L675 (1986).
- [19] F. Greil, B. Drossel, J. Sattler, *New J. Phys.* **9**, 373 (2007).
- [20] F. Greil and B. Drossel, *Phys. Rev. Lett.* **95**, 048701 (2005).
- [21] K. Klemm, S. Bornholdt, H. G. Schuster, *Phys. Rev. Lett.* **84**, 3013 (2000).
- [22] H. J. Kappen and J. Spanjers, *Phys. Rev. E* **61**, 5658 (2000).
- [23] A. Crisanti and H. Sompolinsky, *Phys. Rev. A* **37**, 4865 (1988).
- [24] R. Glauber, *J. Math. Phys.* **4**, 294 (1963).
- [25] M. Suzuki and R. Kubo, *J. Phys. Soc. Jpn.* **24**, 51 (1968).
- [26] D. J. Thouless, P. W. Anderson, R. G. Palmer, *Philos. Mag.* **35**, 593 (1977).
- [27] E. Marinari and V. V. Kerrebroeck, *J. Stat. Mech.: Theory Exp.* P02008 (2010).
- [28] E. Aurell, C. Ollion, Y. Roudi, *Eur. Phys. J. B* **77**, 587 (2010).
- [29] Y. Roudi and J. Hertz, arXiv: 1009.5946v1 (2010).
- [30] Y. Kuramoto and I. Nishikawa, *J. Stat. Phys.* **49**, 569 (1987).